IUTAM Symposium on Unsteady Separated Flows and their Control, June 18-22, 2007, Corfu, Greece

AXISYMMETRIC ABSOLUTE INSTABILITY OF SWIRLING JETS

J. J. HEALEY
Department of Mathematics, Keele University, Keele, Staffs., ST5 5BG, UK
j.j.healey@maths.keele.ac.uk

Abstract

The flow separating from a wing-tip undergoes a vigorous swirling motion, and for large aeroplanes these trailing vortices are strong and persistent and represent a hazard to following aircraft. The resulting flow is characterized by the presence of both axial and azimuthal velocity components. This study is concerned with understanding the instabilities of unsteady disturbances added to such flows. In particular, the absolute/convective instability characteristics of a family of model basic flow profiles to axisymmetric inviscid disturbances is investigated. The new result is that these flows can be absolutely unstable to axisymmetric waves. If the onset of axisymmetric absolute instability turns out to be related to the appearance of axisymmetric vortex breakdown, then these results could provide guidance for how a trailing vortex might be modified to promote vortex breakdown and thereby greatly enhance its dissipation.

1. Introduction

This paper is concerned with the instabilities of swirling jets. In particular, the propagation characteristics of inviscid unstable axisymmetric waves are determined. Swirling jets arise in diverse technological applications. The swirl might be introduced as part of a flow control strategy, or could occur naturally in the flow. Swirling wakes, like trailing wing-tip vorticies, are included implicitly, because they are swirling jets when viewed in the appropriate reference frame. This investigation is motivated by the phenomenon of vortex breakdown of swirling jets in which an axisymmetric bubble of recirculating fluid, with front and rear stagnation points, spontaneously appears in the fluid. This bubble acts like a bluff-body and the wake-like flow behind it breaks down via helical modes. This proceedings paper summarizes findings from a paper recently submitted by the author to the Journal of Fluid Mechanics, and further details can be found there.

Vortex breakdown was first observed in the flow over delta wings in the late 1950s. Harvey (1962) showed how it could be conveniently studied in swirling flows in pipes, and many remarkable flow visualisations of vortex breakdown can be seen in Sarpkaya(1971). Harvey (1960) suggested that it arises by a similar mechanism to that which produces hydraulic jumps in the flow of shallow water. Benjamin (1962) developed a theoretical framework for describing vortex breakdown, like a hydraulic jump, as the transition region connecting an upstream super-critical flow, where all disturbances travel downstream only, to a downstream sub-critical flow, where disturbances can travel upstream and downstream. Benjamin was careful to distinguish his theory from rival theories that proposed that vortex breakdown is the outcome of a hydrodynamic instability of the basic swirling jet flow. Benjamin argued that the super- or sub-critical state of the flow is determined by the propagation properties of neutral inviscid inertial waves, and presented a criterion for the existence of a linearized wave with zero phase velocity, which separates super- from sub-critical flows.

However, swirling jets and wakes also bear unstable waves. The generalization to include the propagation properties of instability waves requires the use of Briggs (1964)'s method to distinguish between convectively unstable flows, where all disturbances travel downstream, as in super-critical flow, and absolutely unstable flows, where disturbances travel upstream and downstream, as in sub-critical flow. See Huerre & Monkewitz (1985) for an early application of Briggs' method to fluid flows, and the review by Huerre & Monkewitz (1990). However, the essential physical concepts of absolute and convective instabilities were independently presented in the context of fluid mechanics by Gaster (1968).

Absolute instability is identified by considering the wavepacket response to an impulsive disturbance to an otherwise undisturbed basic flow. This response can be obtained by evaluating inverse Fourier-Laplace-type transforms over frequencies and wavenumbers. The frequency (Laplace-type) transform is evaluated by placing the integration path above singularities in the complex frequency-plane to respect the principle of causality, i.e. to ensure zero response before introduction of the impulse, then closing the path in the lower half-plane allows residue theory to be used. The problem is thus reduced to an integral in the wavenumber plane, and the integration path is placed on the real axis. At large times this integral can be estimated by deforming the integration path to cross the highest saddle-point whose valleys contain the real axis. This dominant saddle is the pinch-point of Briggs' method. If the imaginary part of the frequency at the pinch-point is positive in the rest-frame then the flow is absolutely unstable. For the axisymmetric jets considered here, it is the axial wavenumber plane that is of interest; the azimuthal wavenumber is an integer. In this paper we restrict attention to axisymmetric waves with zero azimuthal wavenumber.

A number of authors, e.g., Billant, Chomaz & Huerre (1998), Delbende, Chomaz & Huerre (1998), Lim & Redekopp (1998), Loiseleux, Chomaz & Huerre (1998), Olendraru *et al.* (1999), Gallaire & Chomaz (2003a, b), Ruith *et al.* (2003), Gallaire *et al.* (2006) have investigated the possibility of relating the onset of vortex breakdown to the onset of a transition of the jet from a convectively unstable state to an absolutely unstable state. Afterall, it seems reasonable that if a jet supports unstable waves, then it may be their propagation characterstics that determine the appearance of vortex breakdown, because they are expected to dominate the flow field. A lot of progress has been made in establishing a relation between the appearance of helical modes in experiments and simulations with the discovery of absolutely unstable helical modes in the wake region downstream of a nominally axisymmetric breakdown bubble.

However, spatio-temporal stability studies of axisymmetric modes in swirling jets have proved more problematic, and there are no reports of absolutely unstable axisymmetric waves. Lim & Redekopp (1998) calculated the dominant saddle (pinch-point) for axisymmetric inviscid waves in a simple model swirling jet, and found these waves to be convectively unstable. They found that increasing the swirl reduces the damping rate of axisymmetric waves in the rest-frame, but also causes the dominant saddle-point to cross into the left half of the complex wavenumber plane. Such modes appear unphysical because they grow exponentially in the radial direction, while the imposition of homogeneous boundary conditions requires exponential decay of disturbances in the radial direction. This behaviour has presented an obstacle to the use of Briggs' method in the study of axisymmetric waves in swirling jets. However, in the present paper, we show that an understanding of the physical significance of these waves does lead to new insights into the nature of the absolute instability of axisymmetric waves in swirling jets.

In § 2 we review the recently discovered physical interpretation, and consequences, of modes that cross into the left half of the complex wavenumber plane. The governing equations, swirling jet models and dispersion relations are given in § 3. The main results are presented in § 4, and conclusions in § 5.

2. Left half-plane modes

In an unconfined flow the shear layer (jet, wake, boundary layer etc) is surrounded by fluid with constant (possibly zero) velocity. In this outer fluid homogeneous boundary conditions on disturbances require disturbances to decay exponentially with distance from the shear layer. However, if a saddle point approaches the imaginary axis of the wavenumber plane, then its rate of decay in the cross-flow direction diminishes. A saddle point on the imaginary axis does not decay, but has constant amplitude. A saddle point that crosses into the left half of the complex wavenumber plane will grow exponentially in the cross-flow direction. As well as in the swirling-jet study of Lim & Redekopp (1998), left half-plane modes have also been found in mixing layers (Huerre & Monkewitz, 1985) and plane wakes and jets with variable density (Yu & Monkewitz, 1990, Juniper & Candel, 2003, Juniper, 2006), but they were dismissed as unphysical.

However, Healey (2006a) has shown that the pinch-point of the absolute instability in the rotating disk boundary layer becomes asymptotically close to the imaginary axis of the appropriate complex wavenumber plane in the long-wave limit in the inviscid stability problem. The basic flow was von Kármán's similarity profile, which is an exact solution of the Navier-Stokes equations. The stability results were obtained analytically using matched asymptotic expansions and are a self-consistent approximation to the Navier-Stokes equation. It was confirmed that they give accurate quantitative predictions when compared with numerical solutions to the stability equations. Therefore, pinch-points approaching the left half of the complex wavenumber plane are genuine features of spatio-temporal hydrodynamic stability investigations, and require physical interpretation.

A global investigation of the wavenumber plane was needed, which was beyond the scope of the long-wave theory described above. This was carried out by Healey (2006b). It was discovered that there are unstable modes that grow exponentially in the wall-normal direction in the rotating disk boundary layer when the wavenumbers are small enough. These modes are efficiently described using parts of the dispersion relation continued into the left half-plane. Although these roots of the dispersion relation grow exponentially, and are indeed unbounded in the wall-normal direction, and therefore do not satisfy homogeneous boundary conditions, the physical disturbance produced by an initial-value problem does always satisfy homogeneous boundary conditions. This is because the flow field is initially undisturbed, and the disturbance created by forcing at the wall only propagates in the wall-normal direction at finite velocities. The wall-normal propagation velocities can be predicted using a saddle-point method incorporating terms corresponding to propagation in both the streamwise and wall-normal directions (by combining the 'wavy' complex exponential with the exponential form of the eigenfunction taken by the disturbance where the basic flow is uniform). These saddle-points can exist in either the left or right hand halves of the complex plane, but their large-time predictions of wall-normal exponential growth and propagation agree well with numerical evaluations of the inverse transforms calculated using integration paths that pass only over sheets of the dspersion relation that decay exponentially in the wall-normal direction. The part of the dispersion relation that controls the wall-normal growth and propagation has also been described by long-wave theory, see Healey (2005).

The physical behaviour of wall-normal growth and propagation associated with a pinch-point crossing into the left half-plane is sensitive to how the flow is confined in the wall-normal direction. One can normally assume that if the boundary to the flow in the cross-flow direction is far enough away, then the exponential decay of disturbances in the cross-flow direction allows the flow to be treated as unconfined in that direction. However, this is not the case for flows that generate exponential growth in the cross-flow direction: no matter how far away the outer boundary is placed, it still quantitatively, and qualitatively, affects the spatio-temporal stability properties of the flow, as first shown by Healey (2007). Disturbances grow in the wall-normal direction in accordance with the unconfined-flow theory until they reach the outer boundary. There is then a period of reflections of the disturbance between the boundary layer plate and the outer plate while a standing wave is established. At large times, when the outer plate is far from the boundary layer, this standing wave has absolute instability growth rate equal to the maximum growth rate of the wall-normal propagating disturbance of the unconfined flow. Moving the outer plate closer to the shear layer actually increases the absolute instability growth rate (unless the outer plate becomes very close to the shear layer). Therefore, confinement can, in principle, create an absolutely unstable flow from one that would only be convectively unstable when unconfined. These conclusions all follow from the fact that confining a flow is a singular perturbation since the continuous spectrum arising from a branch-cut of the dispersion relation for the unconfined flow is replaced by an infinite discrete spectrum for the confined flow, and Healey (2007) has shown how this leads to infinitely many new saddle-points being created, one of which can form the new pinch-point. The results of Lim & Redekopp (1998), Juniper & Candel (2003) and Juniper (2006) concerning the effect of confinement in problems with pinch-points approaching, or crossing into, the left half-plane are all consistent with the framework developed in Healey (2006b) and Healey (2007), though the implications of a pinch-point entering the left half-plane, and the expected consequences of confinement on the absolute instabilities, were not understood at the time.

We show below that these conclusions carry over directly to the swirling jet problem.

3. Governing equations

The dimensional equations of motion for axisymmetric incompressible inviscid flow in cylindrical coordinates are

$$\frac{1}{r_*}\frac{\partial(r_*u_*)}{\partial r_*}+\frac{\partial w_*}{\partial z_*} = 0 \tag{1}$$

$$\frac{\partial u_*}{\partial t_*}+u_*\frac{\partial u_*}{\partial r_*}+w_*\frac{\partial u_*}{\partial z_*}-\frac{v_*^2}{r_*} = -\frac{1}{\rho_*}\frac{\partial p_*}{\partial r_*} \tag{2}$$

$$\frac{\partial v_*}{\partial t_*}+u_*\frac{\partial v_*}{\partial r_*}+w_*\frac{\partial v_*}{\partial z_*}+\frac{u_*v_*}{r_*} = 0 \tag{3}$$

$$\frac{\partial w_*}{\partial t_*}+u_*\frac{\partial w_*}{\partial r_*}+w_*\frac{\partial w_*}{\partial z_*} = -\frac{1}{\rho_*}\frac{\partial p_*}{\partial z_*} \tag{4}$$

where the radial and axial coordinates are r_* and z_* respectively, time is t_* and ρ_* is the density of the fluid. The velocities in the radial, azimuthal and axial directions are u_*, v_* and w_* respectively and the pressure is p_*. Lengths are made dimensionless using the radius of the jet, R, velocities are made dimensionless using the axial velocity of the jet on the jet axis, U_0, and time by R/U_0. The dimensionless basic flow velocity and pressure profiles for a columnar vortex are $U(r)=0$, $V(r)$, $W(r)$ and $P(r)$, where $\partial P/\partial r = V^2/r$, and the flow field is expressed as a superposition of this basic flow and small unsteady disturbances in the form

$$u_*(r_*,z_*,t_*) = \epsilon U_0 u(r)\exp\mathrm{i}(kz-\omega t), \tag{5}$$

$$v_*(r_*,z_*,t_*) = U_0V(r)+\epsilon U_0 v(r)\exp\mathrm{i}(kz-\omega t), \tag{6}$$

$$w_*(r_*,z_*,t_*) = U_0W(r)+\epsilon U_0 w(r)\exp\mathrm{i}(kz-\omega t), \tag{7}$$

$$p_*(r_*,z_*,t_*) = \rho_*U_0^2P(r)+\epsilon\rho_*U_0^2 p(r)\exp\mathrm{i}(kz-\omega t), \tag{8}$$

which, when substituted into (1) – (4), and linearized in the small parameter ϵ, gives

$$u'+\frac{u}{r}+\mathrm{i}kw = 0, \tag{9}$$

$$-\mathrm{i}\omega u+\mathrm{i}kWu-\frac{2V}{r}v = -p', \tag{10}$$

$$-\mathrm{i}\omega v+\mathrm{i}kWv+V'u+\frac{V}{r}u = 0, \tag{11}$$

$$-\mathrm{i}\omega w+\mathrm{i}kWw+W'u = -\mathrm{i}kp. \tag{12}$$

3.1. A model swirling jet with discontinuous velocity profiles

We re-examine one of the basic flows studied by Lim & Redekopp (1998) in which a jet in rigid-body rotation, and with uniform axial velocity, is surrounded by still fluid of the same density. The dimensionless basic flow is

$$V(r) = \begin{cases} Sr & \text{for} \quad 0 \le r \le 1 \\ 0 & \text{for} \quad r > 1 \end{cases}, \quad W(r) = \begin{cases} 1 & \text{for} \quad 0 \le r \le 1 \\ 0 & \text{for} \quad r > 1 \end{cases}. \tag{13a, b}$$

The swirl, $S = \Omega R/U_0$, measures the azimuthal velocity at the jet edge relative to the axial velocity, where Ω is the angular velocity of the jet. This basic flow is a simple model for the experiment of Billant *et al.* (1998).

Substituting (13) into (9) – (12) and eliminating u, v and w for $0 \le r \le 1$ gives

$$p_1'' + \frac{p_1'}{r} + k^2 \left[\frac{4S^2}{(\omega - k)^2} - 1 \right] p_1 = 0 \tag{14}$$

where the subscript '1' denotes a variable in the core of the jet. The solution that is regular at the jet axis is

$$p_1 = J_0(\beta r), \tag{15}$$

where

$$\beta^2 = k^2 \left[\frac{4S^2}{(\omega - k)^2} - 1 \right] \tag{16}$$

and J_m is the order-m Bessel function of the first kind (the solution has been normalized so that the arbitrary multiplicative constant is unity); the choice of square-root in calculating β is irrelevant because J_0 is an even function. The radial component of the disturbance, required later, is recovered from

$$u_1 = \frac{\mathrm{i}k^2}{(\omega - k)\beta^2} p_1'. \tag{17}$$

Substituting (13) into (9) – (12) and eliminating u, v and w for $r > 1$ gives

$$p_2'' + \frac{p_2'}{r} - k^2 p_2 = 0 \tag{18}$$

where the subscript '2' denotes a variable outside the core of the jet. The solution to (18) depends on the choice of outer boundary condition, i.e. on whether the flow is confined or unconfined in the radial direction.

When the flow is radially unconfined, the solution satisfying homogeneous boundary conditions, i.e. that decays exponentially as $r \to \infty$, is

$$p_2 = A K_0 \left(\sqrt{k^2} r \right), \tag{19}$$

where A is a constant of integration, K_m is the order-m modified Bessel function of the second kind and the square-root has positive real part, which implies branch-cuts on the imaginary axes of the complex k-plane. The radial component of the disturbance, required later, is recovered from

$$u_2 = -\frac{\mathrm{i}}{\omega} p_2'. \tag{20}$$

The solutions in the core are matched to those outside the core by satisfying two jump conditions, which leads to the dispersion relation, see Drazin & Reid (1981). The kinematic condition requires the interface to move with the radial velocity in each region; it leads to

$$\frac{u_1(1)}{\omega - k} = \frac{u_2(1)}{\omega}. \tag{21}$$

The dynamic condition requires continuity of pressure across the interface; it leads to

$$p_2(1) = p_1(1) + \frac{\mathrm{i}S^2}{\omega - k} u_1(1), \tag{22}$$

where the second term on the right-hand side of (22) is due to centrifugal effects.

Substituting (15), (17), (19) and (20) into (21) and (22) and eliminating the constant A produces the dispersion relation for axisymmetric waves in the unconfined swirling jet:

$$0 = k^2 S^2 + \beta(\omega - k)^2 \frac{J_0(\beta)}{J_1(\beta)} + \omega^2 \sqrt{k^2} \frac{K_0(\sqrt{k^2})}{K_1(\sqrt{k^2})}. \tag{23}$$

Additional terms appear in the dispersion relation when the stationary outer fluid is confined by an outer cylinder of dimensionless radius h, coaxial with the jet, giving outer boundary condition $u_2(h) = 0$, and therefore $p_2'(h) = 0$ by (20). The solution to (18) is now

$$p_2 = A' \left[I_1\left(\sqrt{k^2} h\right) K_0\left(\sqrt{k^2} r\right) + K_1\left(\sqrt{k^2} h\right) I_0\left(\sqrt{k^2} r\right) \right], \tag{24}$$

where A' is a constant of integration and I_m is the order-m modified Bessel function of the first kind. Substituting (15), (17), (20) and (24) into (21) and (22) and eliminating the constant A' produces the dispersion relation for axisymmetric waves in the confined swirling jet:

$$0 = k^2 S^2 + \beta(\omega - k)^2 \frac{J_0(\beta)}{J_1(\beta)} + \omega^2 \sqrt{k^2} \frac{I_1(\sqrt{k^2} h) K_0(\sqrt{k^2}) + I_0(\sqrt{k^2}) K_1(\sqrt{k^2} h)}{I_1(\sqrt{k^2} h) K_1(\sqrt{k^2}) - I_1(\sqrt{k^2}) K_1(\sqrt{k^2} h)}. \tag{25}$$

Although the model flow (13) allows these analytical dispersion relations to be derived, it is unphysical in that the discontinuities in velocity at the jet edge generate a Kelvin-Helmholtz instability that makes the initial-value problem ill-posed because arbitrarily short length scales are amplified with arbitrarily large growth rates. Therefore, we also consider smooth velocity profiles.

3.2. A MODEL SWIRLING JET WITH SMOOTH VELOCITY PROFILES

We consider the dimensionless model swirling-jet velocity profiles

$$V(r) = \frac{Sr}{2} \left[1 - \operatorname{erf}\left(\frac{r-1}{d} \right) \right], \quad W(r) = \frac{1}{2} \left[1 - \operatorname{erf}\left(\frac{r-1}{d} \right) \right], \tag{26a, b}$$

where

$$\operatorname{erf}(x) = \frac{2}{\sqrt{\pi}} \int_0^x \mathrm{e}^{-t^2}\, \mathrm{d}t \tag{27}$$

is the error function, which has the property $\lim_{x \to \pm\infty} \operatorname{erf}(x) = \pm 1$. These profiles produce shear layers of dimensionless thickness d at the edge of the jet for both axial and azimuthal profiles, and they are exponentially close to (13) when $|r-1|/d$ is large.

Gallaire & Chomaz (2003b) have also considered smooth velocity profiles that decay to zero outside the jet. Their models are more complicated and have a number of parameters that were tuned to give best fit to the experimental profiles of Billant *et al.* (1998). However, (26) captures the essential properties required for present purposes.

The model profiles (26) are substituted into (9) – (12), which are solved numerically with boundary conditions for unconfined flow. An advantage of these profiles is that away from the shear layers at the jet edge, the analytic solutions (15) and (19) apply, and can be used to produce initial conditions for the numerical solution on each side of the shear layer. The linearized equations are solved by integrating (9) – (12) from $r = 1 - 4d$ to $r = 1$, and from $r = 1 + 4d$ to $r = 1$, and the solutions from each side of the shear layer are matched by requiring p/p' to be continuous at $r = 1$, to produce roots of the dispersion relation. To ensure the accuracy of (15) in providing initial conditions at $r = 1 - 4d$ we only consider $0 < d < 1/4$. There is no stiffness in the differential equations even when d is numerically small because the integration range scales with d.

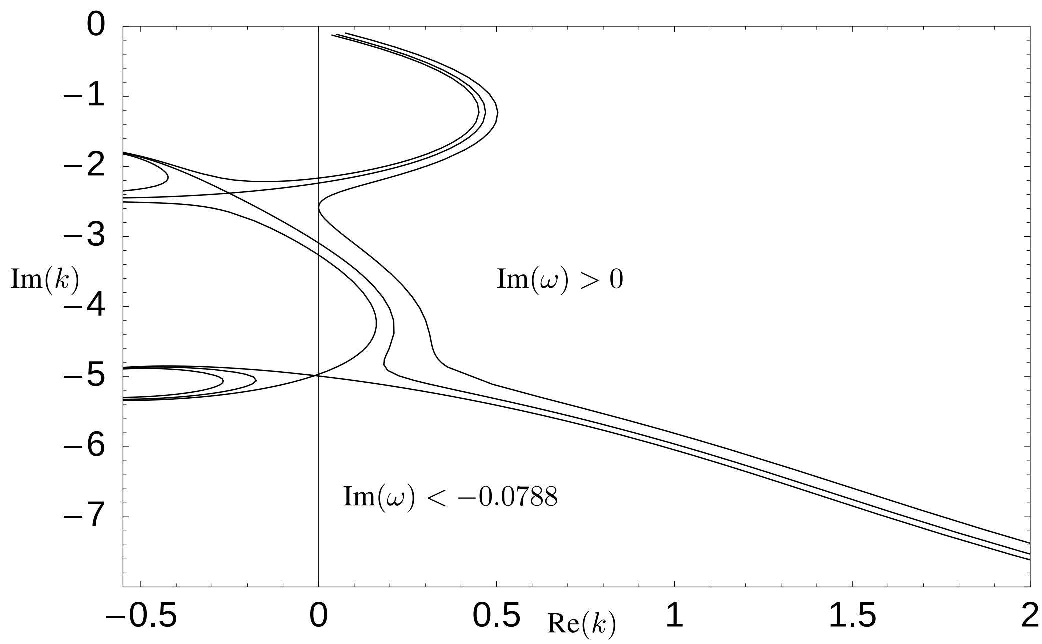

Figure 1. Contours of constant $\mathrm{Im}(\omega)$ in the complex k-plane for the dispersion relation for the unconfined jet (23) for $S = 2.882$. Contours are at $\mathrm{Im}(\omega) = -0.0788$, -0.05074 and 0. The dominant saddle point (pinch-point) lies at $k \approx -0.2514 - 2.382\mathrm{i}$, at which $\omega \approx 3.463 - 0.05074\mathrm{i}$; the other saddle point lies at $k \approx -0.01014 - 4.984\mathrm{i}$, at which $\omega \approx 4.704 - 0.07880\mathrm{i}$. The branch-cut originally placed on the imaginary k-axis has been removed so that solutions with $\mathrm{Re}(k) < 0$ grow exponentially in r as $r \to \infty$, those with $\mathrm{Re}(k) > 0$ decay exponentially in r.

4. Axisymmetric absolute and convective instabilities

The inviscid spatio-temporal stability characteristics of these model swirling jets is determined by plotting contours of constant $\mathrm{Im}(\omega)$ in the complex k-plane. As noted by Lim & Redekopp (1998), the dominant saddle (pinch-point) for the unconfined dispersion relation (23) crosses the imaginary k-axis at $S = 2.203$. However, of particular physical significance is the value $S = 2.882$ at which a contour with $\mathrm{Im}(\omega) = 0$ touches the imaginary k-axis, as shown in figure 1.

For S just larger than 2.882 the $\mathrm{Im}(\omega) = 0$ contour crosses into the left half-plane, but the flow remains convectively unstable, so one could consider the response to periodic forcing. If the forcing frequency is chosen to lie within the range of frequencies for which the $\mathrm{Im}(\omega) = 0$ contour lies in the left half-plane, then the forced response will be a mode that grows exponentially in r for large r. However, at finite times after the forcing is switched on, this mode will only have propagated a finite radial distance. Thus a wave growing exponentially in r can, nonetheless, satisfy homogeneous boundary conditions at all times. The radial propagation of the front of this normal mode is part of the start-up transient created when the periodic forcing is switched on, and it can be determined from a consideration of the impulse response. The standard saddle-point method for calculating the impulse response at large times can be adapted so that propagation in the cross-flow direction, as well as the usual streamwise direction, can be investigated, see Healey (2006b).

However, this growth in the radial direction only continues until the disturbance reaches the boundary of the flow. Ordinarily, a boundary placed far from the jet has little influence on the disturbances within the jet because of their exponential radial decay outside the jet. Conversely, the boundary, however far away, has a major effect on these modes that grow exponentially in the radial direction. The effects of cross-flow confinement on this type of mode were investigated in Healey (2007) for waves in a model of the rotating disk boundary layer. It was shown that con-

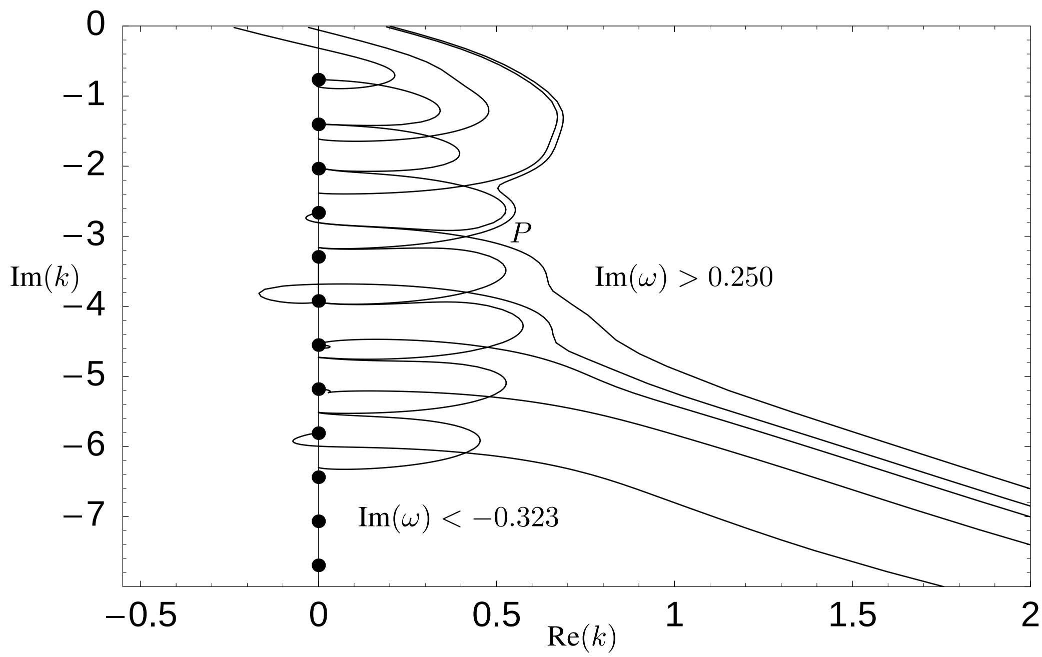

Figure 2. Contours of constant $\mathrm{Im}(\omega)$ in the complex k-plane for the dispersion relation for the confined jet (25) for $S = 2.882$ and $h = 5$. Contours are at the levels of the saddle points created by confinement; the saddles, and $\mathrm{Im}(\omega)$ for each one, in the form $(k, \mathrm{Im}(\omega))$, are at $(0.167 - 0.840\mathrm{i}, -0.319)$, $(0.312 - 1.574\mathrm{i}, -0.056)$, $(0.408 - 2.283\mathrm{i}, 0.228)$, $(0.414 - 3.01\mathrm{i}, 0.250)$, $(0.417 - 3.800\mathrm{i}, 0.171)$, $(0.475 - 4.584\mathrm{i}, 0.121)$, $(0.481 - 5.289\mathrm{i}, -0.009)$ and $(0.414 - 6.090\mathrm{i}, -0.323)$. The dominant saddle point (pinch-point), marked P, lies at $(0.414 - 3.01\mathrm{i}, 0.250)$. The poles, where $\omega \to \infty$, are marked by solid disks.

finement creates an infinite number of new saddle points that approach the imaginary k-axis as the confinement boundary is placed further from the shear layer. Figure 2 shows how confinement by an outer cylinder has the same effect on the complex wavenumber plane for the swirling jet. One of the confinement saddle points becomes the pinch-point, and so confinement creates axisymmetric absolute instability for swirling jets. As $h \to \infty$ the confinement saddles approach the imaginary k-axis, but the confined flow remains absolutely unstable for $S > 2.882$ for arbitrarily large h even though the unconfined flow is only convectively unstable, see the neutral curve for absolute instability in figure 3.

Complex wavenumber planes have also been calculated for the smooth profiles (26). It has been verified that for sufficiently small d the picture approaches that of the discontinuous model (13), and that a short-wave cut-off for the instability is created, producing a well-posed initial-value problem. Furthermore, it is found that increasing d enhances axisymmetric absolute instability via an enhancement of the centrifugal instability present in the shear layers at the jet edge. The rotating core of the jet acts like the rotating inner cylinder of a Taylor-Couette experiment. Figure 4 shows the neutral curve for axisymmetric absolute instability in the unconfined smooth swirling jet.

5. Conclusions

Axisymmetric absolute instability has been found for swirling jet models. It has been shown that confining a swirling jet can create axisymmetric absolute instability even when the unconfined swirling jet is only convectively unstable, and even when the confining outer cylinder has arbitrarily large radius. It is interesting to note that many experiments on vortex breakdown are carried out with swirling jets inside pipes. It may be that confinement inside the pipe enhances the absolute instability which in turn leads to vortex breakdown.

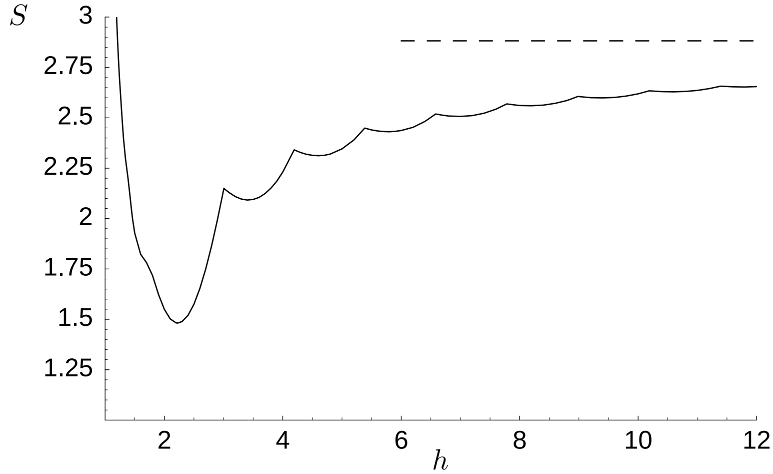

Figure 3. Solid line is neutral curve for absolute instability; dashed line is the asymptote for the neutral curve as $h \to \infty$ at $S = 2.882$ where the $\mathrm{Im}(\omega) = 0$ contour touches the imaginary k-axis in the unconfined problem.

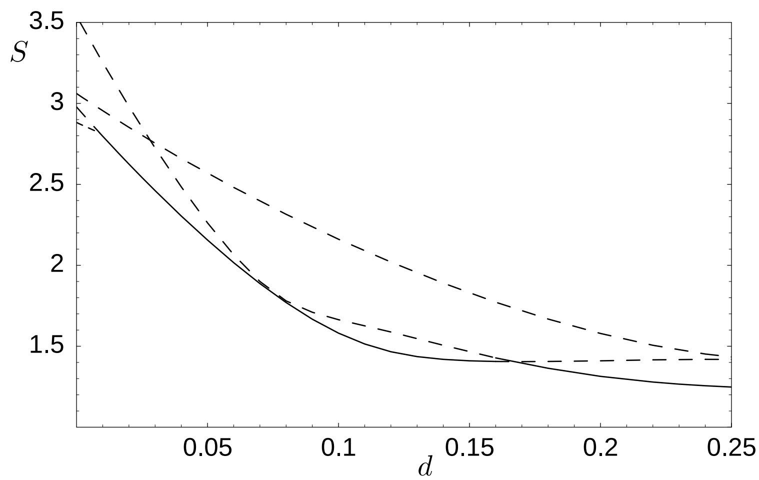

Figure 4. Solid line is neutral curve for absolute instability for the smooth profiles (26) with unconfined flow; dashed lines indicate subdominant saddle-points with $\mathrm{Im}(\omega) = 0$. Values at $d = 0$ were obtained using (23). Eigenvalues at the pinch-points on the neutral curve at $S = 2.5$ are $k \approx 0.265 - 4.92\mathrm{i}$, $\omega \approx 4.03$; at $S = 2$ they are $k \approx 0.674 - 4.88\mathrm{i}$, $\omega \approx 3.26$.

Centrifugal instability acts in the shear layer at the edge of the jet, and is found to enhance the absolute instability as the shear layer thickens. The following scenario can therefore be envisaged: in an experiment on a swirling jet issuing from a nozzle, the jet will have a thin shear layer at its edge, whose thickness will increase with downstream distance by viscous diffusion. The swirl in the jet will be approximately constant. Figure 4 suggests that for $S > 1.5$ the jet will be convectively unstable as it leaves the nozzle, it will remain convectively unstable for some distance downstream, until the shear layer reaches a critical thickness, at which point the jet becomes absolutely unstable to axisymmetric waves.

A location where the flow undergoes a transition from convective to absolute instability provides a site for the appearance of a steep-fronted nonlinear global mode according to Couairon & Chomaz (1999) and Pier, Huerre & Chomaz (2001). It is also a point where the flow changes from a super-critical state, supporting only downstream propagating waves, to a sub-critical state, supporting both upstream and downstream propagating waves, and Benjamin (1962) has argued that such a point is associated with the appearance of vortex breakdown. It is therefore interesting to consider whether axisymmetric vortex breakdown might be related to a nonlinear global mode created by the transition of a columnar vortex from a convectively unstable state to an absolutely unstable state. Typical experimental values for the swirl that triggers vortex breakdown are $S \approx 1.6$, which is certainly consistent with values for axisymmetric absolute instability shown in figures 3 and 4.

REFERENCES

1 BENJAMIN, T. B.: Theory of the vortex breakdown phenomenon. J. Fluid Mech. **14** (1962) 593–629.

2 BILLANT, P., CHOMAZ, J.-M. & HUERRE, P.: Experimental study of vortex breakdown in swirling jets. J. Fluid Mech. **376** (1998) 183–219.

3 BRIGGS, R.J.: *Electron-Stream Interaction with Plasmas.* MIT Press (1964).

4 COUAIRON, A. & CHOMAZ, J.-M.: Fully nonlinear global modes in slowly varying flows. Phys. Fluids **11** (1999) 3688–3703.

5 DELBENDE, I., CHOMAZ, J.-M. & HUERRE, P.: Absolute/convective instabilities in the Batchelor vortex: a numerical study of the linear impulse response. J. Fluid Mech. **355** (1998) 229–254.

6 DRAZIN, P. G. & REID, W. H.: *Hydrodynamic Stability Theory.* CUP (1981).

7 GALLAIRE, F. & CHOMAZ, J.-M.: Instability mechanisms in swirling flows. Phys. Fluids **15** (2003a) 2622–2639.

8 GALLAIRE, F. & CHOMAZ, J.-M.: Mode selection in swirling jet experiments: a linear stability analysis. J. Fluid Mech. **494** (2003b) 223–253.

9 GALLAIRE, F., RUITH, M., MEIBURG, E., CHOMAZ, J.-M. & HUERRE, P.: Spiral vortex breakdown as a global mode. J. Fluid Mech. **549** (2006) 71–80.

10 GASTER, M.: Growth of disturbances in both space and time. Phys. Fluids **11** (1968) 723–727.

11 HARVEY, J. K.: Analysis of the vortex breakdown phenomenon, Part II. Aero. Dept., Imperial Coll., Rep. no. 103 (1960).

12 HARVEY, J. K.: Some observations of the vortex breakdown phenomenon. J. Fluid Mech. **14** (1962) 585–592.

13 HEALEY, J. J.: Long-wave theory for a new convective instability with exponential growth normal to the wall. Phil. Trans. R. Soc. Lond. A **363** (2005) 1119–1130.

14 HEALEY, J.J.: Inviscid long-wave theory for the absolute instability of the rotating-disk boundary layer. Proc. R. Soc. Lond. A **462** (2006a) 1467–1492.

15 HEALEY, J.J.: A new type of convective instability with exponential growth perpendicular to the basic flow. J. Fluid Mech. **560** (2006b) 279–310.

16 HEALEY, J. J.: Enhancing the absolute instability of a boundary layer by adding a far-away plate. J. Fluid Mech. **579** (2007) 29–61.

17 HUERRE, P. & MONKEWITZ, P. A.: Absolute and convective instabilities in free shear layers. J. Fluid Mech. **159** (1985) 151–168.

18 HUERRE, P. & MONKEWITZ, P. A.: Local and global instabilities in spatially developing flows. Ann. Rev. Fluid Mech. **22** (1990) 473–537.

19 JUNIPER, M. P.: The effect of confinement on the stability of two-dimensional shear flows. J. Fluid Mech. **565** (2006) 171–195.

20 JUNIPER, M. P. & CANDEL, S. M.: The stability of ducted compound flows and consequences for the geometry of coaxial injectors. J. Fluid Mech. **482** (2003) 257–269.

21 LIM, D.W. & REDEKOPP, L.G.: Absolute instability conditions for variable density swirling jet flows. Eur. J. Mech. B/Fluids **17** (1998) 165–185.

22 LOISELEUX, T., CHOMAZ, J.-M. & HUERRE, P.: The effect of swirl on jets and wakes: linear instability of the Rankine vortex with axial flow. Phys. Fluids **10** (1998) 1120–1134.

23 OLENDRARU, C., SELLIER, A., ROSSI, M. & HUERRE, P.: Inviscid instability of the Batchelor vortex: Absolute-convective transition and spatial branches. Phys. Fluids **11** (1999) 1805–1820.

24 PIER, B., HUERRE, P. & CHOMAZ, J.-M.: Bifurcation to fully nonlinear synchronized structures in slowly varying media. Physica D **148** (2001) 49–96.

25 RUITH, M. R., CHEN, P., MEIBURG, E. & MAXWORTHY, T.: Three-dimensional vortex breakdown in swirling jets and wakes: direct numerical solution. J. Fluid Mech. **486** (2003) 331–378.

26 YU, M.-H. & MONKEWITZ, P. A.: The effect of nonuniform density on the absolute instability of two-dimensional inertial jets and wakes. Phys. Fluids A **2** (1990) 1175–1181.